Depairing Current Density in Superconductors

Teruo Matsushita and Masaru Kiuchi

Department of Computer Science and Electronics, Kyushu Institute of Technology, Iizuka, Fukuoka 820-8502, Japan

*E-mail: matsushita.teruo391@mail.kyutech.jp

The depairing current density in superconductors is theoretically investigated for magnetization and transport currents. It is found that the depairing current densities in both cases are higher than those predicted by Tinkham. One of the reasons for the higher current densities is that those are obtained at the transition point to the normal state, while Tinkham obtained in the superconducting state far from the transition boundary. Another reason is that the order parameter is larger than the equilibrium value, which contributes not only directly to a higher current density but also to a lower kinetic energy due to the current.

Recently, artificial pinning centers have been commonly introduced into $REBa_2Cu_3O_{7-\delta}$ (REBCO) superconducting films to improve the critical current density.[1)] In this case, of great interest is the attainable critical current density, and the observed results are frequently compared with the depairing current density.[2)]

The depairing current density is the maximum microscopic current density attained in superconductors with transverse sizes smaller than the coherence length. Hence, the spatial variation in the order parameter can be neglected. Using the London model the depairing current density was theoretically determined at the transition point to the normal state, at which the kinetic energy density due to the current is equal to the absolute value of the condensation energy density.[3)] The predicted depairing current density is given by

$$j_{\mathrm{d0}} = \frac{H_{\mathrm{c}}}{\lambda}. \tag{1}$$

Here, H_{c} is the thermodynamic critical field and λ is the penetration depth given by

$$\lambda = \left(\frac{m^*}{4\mu_0 e^2 |\Psi_\infty|^2} \right)^{1/2}, \tag{2}$$

where $-2e(e > 0)$ and m^* are the electric charge and mass of a superconducting electron, respectively, and $|\Psi_\infty|^2$ is the equilibrium value of the order parameter. Tinkham[4)] estimated the depairing current density assuming the velocity of a superconducting electron v_{s} as one of the internal variables and obtained

$$j_{\mathrm{d}}' = \left(\frac{2}{3}\right)^{3/2} \frac{H_{\mathrm{c}}}{\lambda} \cong 0.5443 \frac{H_{\mathrm{c}}}{\lambda}. \tag{3}$$

The reduction from the result in Eq. (1) was attributed to the decrease in the order parameter $|\Psi|^2$ from $|\Psi_\infty|^2$. These results are applicable to the case of induced magnetization current. In the case of transport current, the Gibbs free energy density was considered and Tinkham again obtained Eq. (3).

The depairing current density may be attained only for very thin superconductors such as nanowhiskers, and it is difficult to obtain sufficiently large superconducting currents because of the limited cross-sectional areas. The mechanism of the limiting current is completely different from that of the macroscopic critical current density for practical applications based on the flux pinning mechanism. Thus, the attainable value of the pinning critical current density for superconductors with much larger cross-sectional areas was theoretically investigated. The obtained result was[5)]

$$J_{\mathrm{c}} = 0.6712\frac{H_{\mathrm{c}}}{\lambda}, \tag{4}$$

which is larger than that in Eq. (3). However, it is difficult to understand why the obtained critical current density at which the resistive flux flow state starts can be higher than the microscopic critical current density at which the superconductivity is destroyed. In the theoretical treatment in Ref. 4, the order parameter was smaller than the equilibrium value, as mentioned above. This is disadvantageous, however, since it reduces the current density and increases the kinetic energy. On the other hand, the higher maximum pinning critical current density than that predicted by Tinkham is attributed to the larger order parameter. In this paper, therefore, the theoretical treatment in Ref. 4 is reexamined in detail in the cases of both magnetization and transport currents.

Since the spatial variation in the order parameter can be neglected in the thin superconductor, the Ginzburg-Landau energy density is simply given by

$$\mathcal{F} = \alpha|\Psi|^2 + \frac{1}{2}\beta|\Psi|^4 + \frac{m^* j^2}{8e^2|\Psi|^2}. \tag{5}$$

The third term is the kinetic energy density due to the current. The reason why the description of the energy density is different from that in Ref. 4 will be discussed later. Minimizing $\mathcal{F}$ with respect to $|\Psi|^2$ under a given current density j, we obtain

$$\alpha + \beta|\Psi|^2 - \frac{m^* j^2}{8e^2|\Psi|^4} = 0. \tag{6}$$

Using the relationships $|\Psi_\infty|^2 = -\alpha/\beta$ and $(|\alpha|/m^*)^{1/2} = j_{d0}/2e|\Psi_\infty|^2$, Eq. (6) is reduced to

$$\left(\frac{j}{j_{d0}}\right)^2 = 2\left(\frac{|\Psi|^2}{|\Psi_\infty|^2}\right)^3 - 2\left(\frac{|\Psi|^2}{|\Psi_\infty|^2}\right)^2. \tag{7}$$

This shows that the order parameter takes a value larger than the equilibrium value ($|\Psi|^2 \geq |\Psi_\infty|^2$), the same trend as in the case of the macroscopic pinning current density[5)] but this trend is opposite to that obtained from the theoretical treatment in Ref. 4. Since the order parameter increases monotonically from the equilibrium value with increasing current density, resulting in an increase in negative condensation energy density, which is equal to the sum of the first and second terms in Eq. (5), the maximum superconducting current density is considered to be obtained at the transition to the normal state ($\mathcal{F}$ =0). This condition is written as

$$\left(\frac{j}{j_{d0}}\right)^2 = -\left(\frac{|\Psi|^2}{|\Psi_\infty|^2}\right)^3 + 2\left(\frac{|\Psi|^2}{|\Psi_\infty|^2}\right)^2. \tag{8}$$

From Eqs. (7) and (8), the maximum current density is obtained at $|\Psi|^2/|\Psi_\infty|^2 = 4/3$. That is, the depairing current density is

$$j_d = 2\left(\frac{2}{3}\right)^{3/2}\frac{H_c}{\lambda} \cong 1.089\frac{H_c}{\lambda}. \tag{9}$$

This is exactly twice the value given by Eq. (3).

In the case of transport current, the Gibbs energy density

$$\mathcal{g} = \mathcal{F} - \boldsymbol{A} \cdot \boldsymbol{j} \tag{10}$$

must be treated under a given current density $\boldsymbol{j}$, where $\boldsymbol{A}$ is the vector potential. Since the spatial variation in the phase of the order parameter can be neglected, from the Ginzburg-Landau equation we have

$$\boldsymbol{A} = -\frac{m^* \boldsymbol{j}}{4e^2 |\Psi|^2}. \tag{11}$$

Thus, the Gibbs free energy density is given by

$$\mathcal{g} = \alpha |\Psi|^2 + \frac{1}{2} \beta |\Psi|^4 + \frac{3m^* j^2}{8e^2 |\Psi|^2}. \tag{12}$$

Minimizing $\mathcal{g}$ with respect to $|\Psi|^2$, we obtain

$$\left(\frac{j}{j_{\mathrm{d0}}}\right)^2 = \frac{2}{3}\left(\frac{|\Psi|^2}{|\Psi_\infty|^2}\right)^3 - \frac{2}{3}\left(\frac{|\Psi|^2}{|\Psi_\infty|^2}\right)^2. \tag{13}$$

The order parameter again takes a value larger than the equilibrium value. The maximum current density is similarly expected to be obtained at the transition point to the normal state. Since the magnetic condition does not change at the transition, the Legendre term, $-\boldsymbol{A} \cdot \boldsymbol{j}$, is unchanged. This will be shown below.

We assume for simplicity that a current is applied to a very thin superconductor ($-d \le x \le d$) along the z-axis. In the superconducting state, the current is distributed in the superconductor with a density of

$$j_z(x) = j_0 \cosh\frac{x}{\lambda'}, \tag{14}$$

where λ' is the penetration depth given by

$$\lambda' = \left(\frac{m^*}{4\mu_0 e^2 |\Psi|^2}\right)^{1/2}. \tag{15}$$

Note that λ' is not equal to the London penetration depth given by Eq. (2). Hence, using the Maxwell equations, the magnetic flux density has the y-component

$$\frac{\partial B_y}{\partial x} = \mu_0 j_z, \tag{16}$$

which leads to

$$B_y = \mu_0 \lambda' j_0 \sinh\frac{x}{\lambda'}. \tag{17}$$

Then, from the relationship

$$\frac{\partial A_z}{\partial x} = -B_y, \tag{18}$$

the vector potential is obtained as

$$A_z = -\mu_0 \lambda'^2 j_0 \cosh\frac{x}{\lambda'} = -\mu_0 \lambda'^2 j_z. \tag{19}$$

This is the same as Eq. (11). Because $d \ll \lambda'$, the current density and vector potential are almost spatially uniform inside the superconductor. The nonuniformity of each quantity is on the order of $(d/\lambda')^2$ in magnitude and we can safely neglect such nonuniformities. When the current density on the surface of the superconductor reaches the critical value j_d, the transition to the normal state occurs.

In the normal state, the current density is completely uniform inside the superconductor and this is almost equal to that in the superconducting state. As a result, the resultant magnetic flux density and vector potential are also almost the same as those in the superconducting state. In fact, from Eq. (16), the magnetic flux density is

$$B_y = \mu_0 j_d x. \tag{20}$$

From Eq. (18), the vector potential is obtained as

$$A_z = K - \frac{1}{2}\mu_0 j_d x^2, \tag{21}$$

where K is a constant value. We can assume K to be equal to the constant value in the superconducting state with a suitable gauge. The nonuniformity given by the second term is relatively on the order of $(d/\lambda')^2$ in magnitude and can be safely neglected. Hence, the vector potential is substantially the same as that in the superconducting state. This is natural since the current distribution does not change appreciably upon the transition to the normal state. Thus, it can be concluded that the Legendre term is continuous at the transition point.

Hence, the transition occurs when $\mathcal{F}$ reaches zero. This is similar to the transition to the normal state at the upper critical field,[6] H_{c2}. This condition is given by Eq. (8). From Eqs. (8) and (13), we obtain $|\Psi|^2/|\Psi_\infty|^2 = 8/5$ and the depairing current density

$$j_d = 4\left(\frac{2}{5}\right)^{3/2}\frac{H_c}{\lambda} \cong 1.012\frac{H_c}{\lambda}. \tag{22}$$

This value is slightly smaller than that in Eq. (9) but is larger than that in Eq. (3).

Here we discuss the obtained results. First, we focus on the result for the magnetization current. In Ref. 4, the Ginzburg-Landau energy density was described as

$$\mathcal{F} = \alpha|\Psi|^2 + \frac{1}{2}\beta|\Psi|^4 + \frac{1}{2}m^*|\Psi|^2{v_\mathrm{s}}^2 \tag{23}$$

in terms of the order parameter $|\Psi|^2$ and the velocity of a superconducting electron, v_s, which are independent of each other. The velocity of a superconducting electron is related to the current density as

$$j = -2e|\Psi|^2 v_\mathrm{s}. \tag{24}$$

Minimizing Eq. (23) with respect to $|\Psi|^2$ leads to

$$\alpha + \beta|\Psi|^2 + \frac{1}{2}m^*{v_\mathrm{s}}^2 = 0. \tag{25}$$

This shows that $|\Psi|^2$ is smaller than $|\Psi_\infty|^2$. Equation (25) is written as

$$\left(\frac{m^*}{|\alpha|}\right)^{1/2} v_\mathrm{s} = -\left[2\left(1 - \frac{|\Psi|^2}{|\Psi_\infty|^2}\right)\right]^{1/2}. \tag{26}$$

In Ref. 4, the maximum current density given by Eq. (3) was obtained at $|\Psi|^2/|\Psi_\infty|^2 = 2/3$ under the condition of Eq. (26).

Figure 1 shows a contour map of the normalized Ginzburg-Landau energy density given by

$$f = (|\alpha||\Psi_\infty|^2)^{-1}\mathcal{F} = -\frac{|\Psi|^2}{|\Psi_\infty|^2} + \frac{1}{2}\left(\frac{|\Psi|^2}{|\Psi_\infty|^2}\right)^2 + \frac{1}{2}\left(\frac{|\Psi|^2}{|\Psi_\infty|^2}\right)^{-1}\left(\frac{j}{j_\mathrm{d0}}\right)^2 \tag{27}$$

$$= -\frac{|\Psi|^2}{|\Psi_\infty|^2} + \frac{1}{2}\left(\frac{|\Psi|^2}{|\Psi_\infty|^2}\right)^2 + \frac{1}{2}\frac{|\Psi|^2}{|\Psi_\infty|^2}\left[\left(\frac{m^*}{|\alpha|}\right)^{1/2} v_\mathrm{s}\right]^2$$

on the normalized order parameter ($|\Psi|^2/|\Psi_\infty|^2$) vs velocity ($(m^*/|\alpha|)^{1/2}|v_\mathrm{s}|$) plane that was treated in Ref. 4. This clearly shows that there is no true local minimum point of the energy density. That is, although the energy density has a minimum value on the line given by Eq. (26) when the order parameter changes under a fixed velocity value, the free energy density monotonically decreases when the velocity decreases along this line. Hence, there is no reason to restrict ourselves only to the superconducting states on the line when searching for the maximum current density. The minimization of the energy density given by Eq. (23) is meaningless for this purpose. On the other hand, this theoretical process is useful for investigating the value of velocity. In fact, $(m^*/|\alpha|)^{1/2}|v_\mathrm{s}|$ takes a value from 0 to $\sqrt{2}$, the maximum value, along the broken line determined by Eq. (26).

The maximum current density must be searched for throughout the area of the superconducting state, which is the region to the left of the line $f = 0$ in Fig. 1. Note that the value of the normalized velocity is the same ($(m^*/|\alpha|)^{1/2}|v_\mathrm{s}| = (2/3)^{1/2}$) for the present critical point corresponding to Eq. (9) and that in Ref. 4. The difference in depairing current density by a factor of 2 directly originates from the difference in the order parameter. The discussion in the previous paragraph indicates that it is not necessary to restrict the combination of variables to the order parameter and velocity, which are independent of each other, to describe the Ginzburg-Landau energy density. For this purpose, each local minimum condition of the energy with respect to $|\Psi|^2$ should be searched for a given j value, then, the maximum j value should be found among the local minimum conditions. This is the reason why we used the Ginzburg-Landau energy density given by Eq. (5). If we minimize Eq. (23) with respect to v_s under the condition of Eq. (24), we have the same result as Eq. (6).

Figure 2 shows a contour map of the normalized Ginzburg-Landau energy density on the normalized order parameter ($|\Psi|^2/|\Psi_\infty|^2$) vs current density (j/j_d0) plane. It is found that the superconducting state is extended to a higher current density for a larger order parameter, which is opposite to the trend shown in Fig. 1. The procedure of minimizing the Ginzburg-Landau energy density given by Eq. (5) is useful for determining the maximum value of j. In fact, Fig. 2 clearly shows that the normalized current density ranges from 0 to $2(2/3)^{3/2}$ along broken line 1 given by Eq. (7). The value given by Eq. (9) is the maximum in the region of the superconducting state. The critical points of the present analysis and the Tinkham and London models are shown in the figure for comparison. The higher depairing current density than that obtained from the London model is also attributed to the larger order parameter.

Next, we discuss the result for the transport current. The Gibbs free energy density assumed in Ref. 4 is

$$g = \alpha|\Psi|^2 + \frac{1}{2}\beta|\Psi|^4 - \frac{m^* j^2}{8e^2|\Psi|^2}. \tag{28}$$

Hence, the Legendre term for the transformation is

$$-\frac{m^* j^2}{4e^2|\Psi|^2} = \boldsymbol{A}\cdot\boldsymbol{j}. \tag{29}$$

However, this should be $-\boldsymbol{A}\cdot\boldsymbol{j}$. This simple mistake led to the underestimation of the depairing current density.

Figure 3 is a replot of Fig. 1 to show the variation in the Ginzburg-Landau energy density f as a function of the order parameter at various values of the current density. It was concluded in Ref. 4 that the critical current density of $j/j_{\rm d0} = (2/3)^{3/2}$ is obtained at $|\Psi|^2/|\Psi_\infty|^2 = 2/3$. The normalized Ginzburg-Landau energy density at this point shown by the open circle is $f = -2/9$. On the other hand, we have a lower energy of $f = -0.3605$ at $|\Psi|^2/|\Psi_\infty|^2 = 1.1184$, as shown by the asterisk in Fig. 3, even though the current flows with the same density ($j/j_{\rm d0} = (2/3)^{3/2}$). In more detail, the normalized condensation energy density f_{c} and kinetic energy density f_{k} are compared between the two cases in Table 1. These energy densities are given by

$$f_{\mathrm{c}} = -\frac{|\Psi|^2}{|\Psi_\infty|^2} + \frac{1}{2}\left(\frac{|\Psi|^2}{|\Psi_\infty|^2}\right)^2 \tag{30}$$

and

$$f_{\mathrm{k}} = \frac{1}{2}\left(\frac{|\Psi|^2}{|\Psi_\infty|^2}\right)^{-1}\left(\frac{j}{j_{\mathrm{d0}}}\right)^2. \tag{31}$$

This clearly shows that the condition in the present analysis is much more convenient from the energetic viewpoint. That is, the degradation of the condensation energy density from the equilibrium value $(-1/2)$ is smaller and the kinetic energy density is lower even for the same current density. This is the reason why the higher depairing current density is obtained. Figure 3 also clearly shows the reason why the obtained depairing current density is even higher than that predicted by the London model.

The locus of the minimum point of the Ginzburg-Landau energy density is obtained by substituting Eq. (7) into Eq. (27) as

$$f_{\mathrm{m}} = \frac{3}{2}\left(\frac{|\Psi|^2}{|\Psi_\infty|^2}\right)^2 - 2\frac{|\Psi|^2}{|\Psi_\infty|^2}. \tag{32}$$

Using Eqs. (13) and (27), the locus of the minimum point of the Gibbs free energy density is

$$f_{\mathrm{m}}' = \frac{5}{6}\left(\frac{|\Psi|^2}{|\Psi_\infty|^2}\right)^2 - \frac{4}{3}\frac{|\Psi|^2}{|\Psi_\infty|^2}. \tag{33}$$

The broken and dot-dashed lines in Fig. 3 are f_{m} and f_{m}', respectively. These minimum points move to a larger order parameter as the current density increases. The respective critical points given by Eqs. (9) and (22) are also shown in the figure. In the case of transport current, the deviation from the locus of the minimum Ginzburg-Landau energy density causes a lower depairing current density.

The theoretical treatment in this study clarifies that the true depairing current densities are higher than the maximum pinning current density. Hence, the results obtained in this study are reasonable.

In summary, the depairing current density was theoretically investigated for magnetization and transport currents in this study. The depairing current density was found to be $2(2/3)^{3/2}H_{\mathrm{c}}/\lambda$ and $4(2/5)^{3/2}H_{\mathrm{c}}/\lambda$, for the magnetization and transport currents, respectively. Both of them are higher than that theoretically predicted by Tinkham and even that by London. Under the condition of Tinkham, the Ginzburg-Landau energy density is negative, indicating that the superconductor is in the superconducting state. On the other hand, the present results were obtained at the transition point to the normal state, and hence the above current densities are indeed the depairing current densities. The enhancement of the order parameter from the equilibrium value contributes to the higher depairing current density. The obtained results are reasonable since the obtained depairing current densities are higher than the maximum pinning current density of $0.6712H_{\mathrm{c}}/\lambda$.

References

1) M. Miura, B. Maiorov, M. Sato, M. Kanai, T. Kato, T. Kato, T. Izumi, S. Awaji, P. Mele, M. Kiuchi, and T. Matsushita, Tuning nanoparticle size for enhanced functionality in perovskite thin films deposited by metal organic deposition, NPG Asia Mater. **9**, e447 (2017) and references therein.

2) See, for example, K. Matsumoto and P. Mele, Artificial pinning center technology to enhance vortex pinning in YBCO coated conductors, Supercond. Sci. Technol. **23**, 014001 (2010).

3) M. N. Kunchur, Current-induced pair breaking in magnesium diboride, J. Phys.: Condens. Matter **16**, R1183 (2004).

4) M. Tinkham, *Introduction to Superconductivity* (McGraw-Hill, New York, 1996) 2nd ed., p. 123.

5) T. Matsushita and M. Kiuchi, Theoretical estimation of the upper limit of critical current density by flux pinning in superconductors under the influence of kinetic energy, Appl. Phys. Express, **12**, 023004 (2019).

6) T. Matsushita, *Flux Pinning in Superconductors* (Springer, Berlin, 2014) 2nd ed., p. 23.

Table 1. Comparison of the normalized energy densities. Two cases are compared at $j/j_{\mathrm{d0}} = (2/3)^{3/2}$. f_c and f_k are the normalized condensation energy density and kinetic energy density, respectively.

	$\lvert\Psi\rvert^2/\lvert\Psi_\infty\rvert^2$	f_c	f_k	f
Present	1.1184	−0.4930	0.1325	−0.3605
Ref. 4	0.6667	−0.4444	0.2222	−0.2222

Figure captions

Fig. 1. Contour map of the normalized Ginzburg-Landau energy density f on the order parameter $(|\Psi|^2/|\Psi_\infty|^2)$ vs superconducting electron velocity $((m^*/|\alpha|)^{1/2}|v_\mathrm{s}|)$ plane. The broken line shows the equilibrium condition given by Eq. (26). The critical point of the present analysis $\left(|\Psi|^2/|\Psi_\infty|^2 = 4/3, (m^*/|\alpha|)^{1/2}|v_\mathrm{s}| = (2/3)^{1/2}\right)$ and that of the Tinkham model $\left(2/3, (2/3)^{1/2}\right)$ are shown.

Fig. 2. Contour map of the normalized Ginzburg-Landau energy density f on the order parameter $(|\Psi|^2/|\Psi_\infty|^2)$ vs superconducting current density (j/j_d0) plane. Broken lines 1 and 2 show the equilibrium conditions of Eq. (7) and (13), respectively, and the dot-dashed line shows the equilibrium value of the order parameter $(|\Psi|^2/|\Psi_\infty|^2 = 1)$. The critical points of the present analysis $\left(|\Psi|^2/|\Psi_\infty|^2 = 4/3, j/j_\mathrm{d0} = 2(2/3)^{3/2}\right)$ and $(8/5, 4(2/5)^{3/2})$ are shown by the solid circles. Those of the Tinkham model $\left(2/3, (2/3)^{3/2}\right)$ and London model (1,1) are also shown by the open circle and triangle, respectively.

Fig. 3. Normalized Ginzburg-Landau energy density f as a function of the order parameter $(|\Psi|^2/|\Psi_\infty|^2)$ at various values of the current density (j/j_d0). f_m and f_m' are the loci of the minimum points of the Ginzburg-Landau and Gibbs free energy densities, respectively. The respective critical points of the depairing current density given by Eq. (9) and (22) are shown by the solid circles. The critical points of the Tinkham and London models are also shown by the open circle and triangle, respectively. The asterisk shows the condition in the present analysis for which current density is the same as the result in Ref. 4.

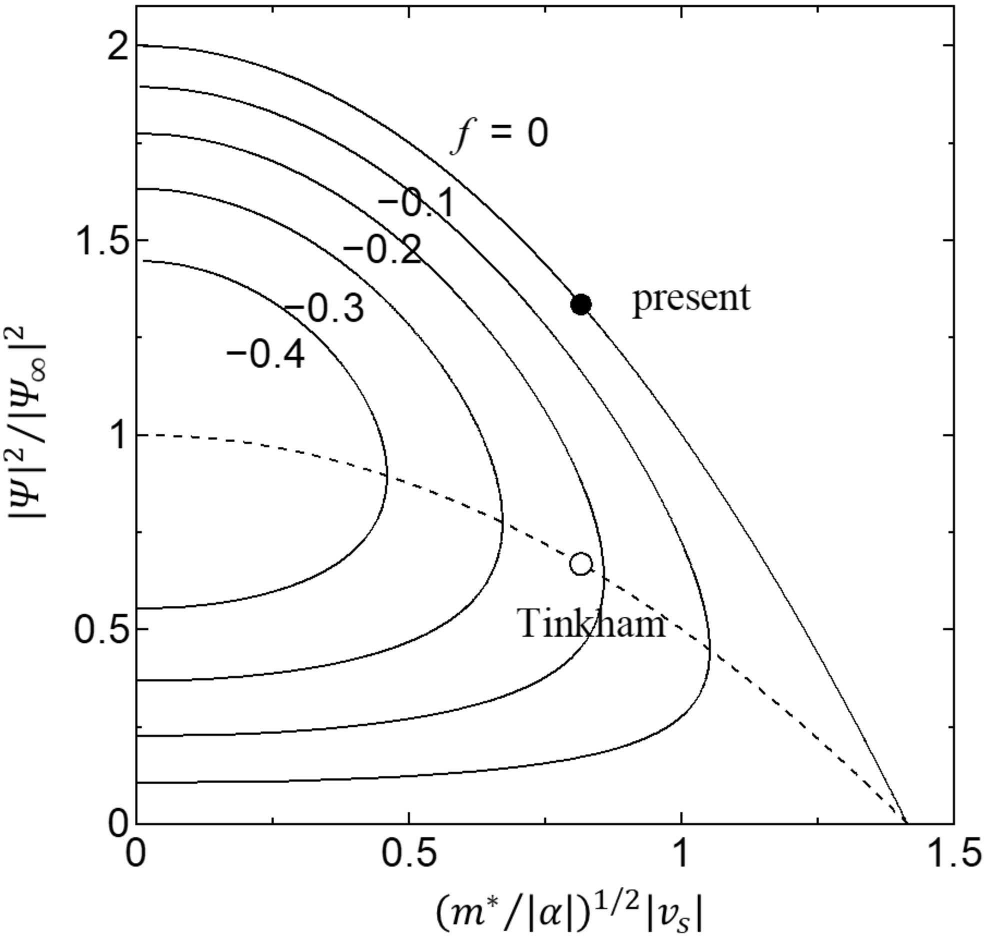

2
1.5
1
0.5
0
0
0.5
1
1.5
$|\Psi|^2/|\Psi_\infty|^2$
$(m^*/|\alpha|)^{1/2}|v_s|$
f = 0
−0.1
−0.2
−0.3
−0.4
present
Tinkham

Fig. 1

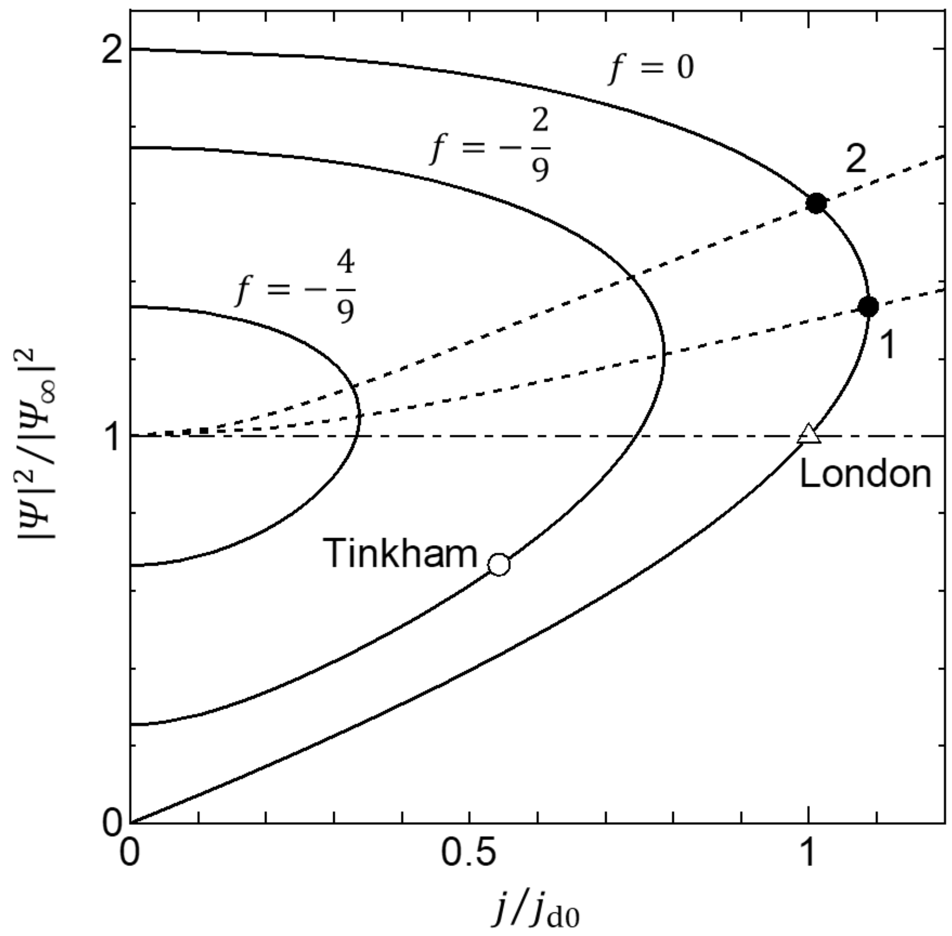

$f = 0$
$f = -\frac{2}{9}$
$f = -\frac{4}{9}$
2
1
London
Tinkham
$|\Psi|^2/|\Psi_\infty|^2$
j/j_{d0}
0
0.5
1
2

Fig. 2

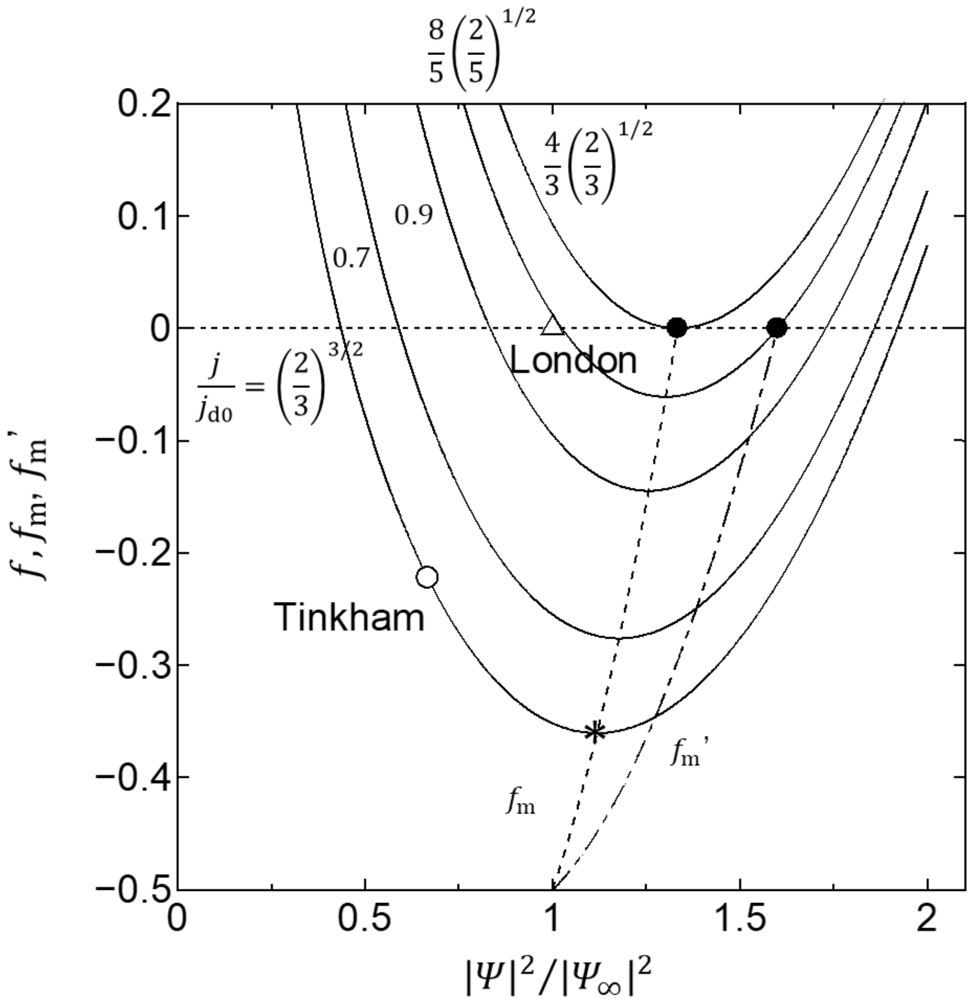

$\frac{8}{5}\left(\frac{2}{5}\right)^{1/2}$
$\frac{4}{3}\left(\frac{2}{3}\right)^{1/2}$
0.9
0.7
London
$\frac{j}{j_{\mathrm{d0}}} = \left(\frac{2}{3}\right)^{3/2}$
Tinkham
f_{m}'
f_{m}
$f, f_{\mathrm{m}}, f_{\mathrm{m}}$'
$|\Psi|^2/|\Psi_\infty|^2$
0.2
0.1
0
−0.1
−0.2
−0.3
−0.4
−0.5
0
0.5
1
1.5
2

Fig. 3